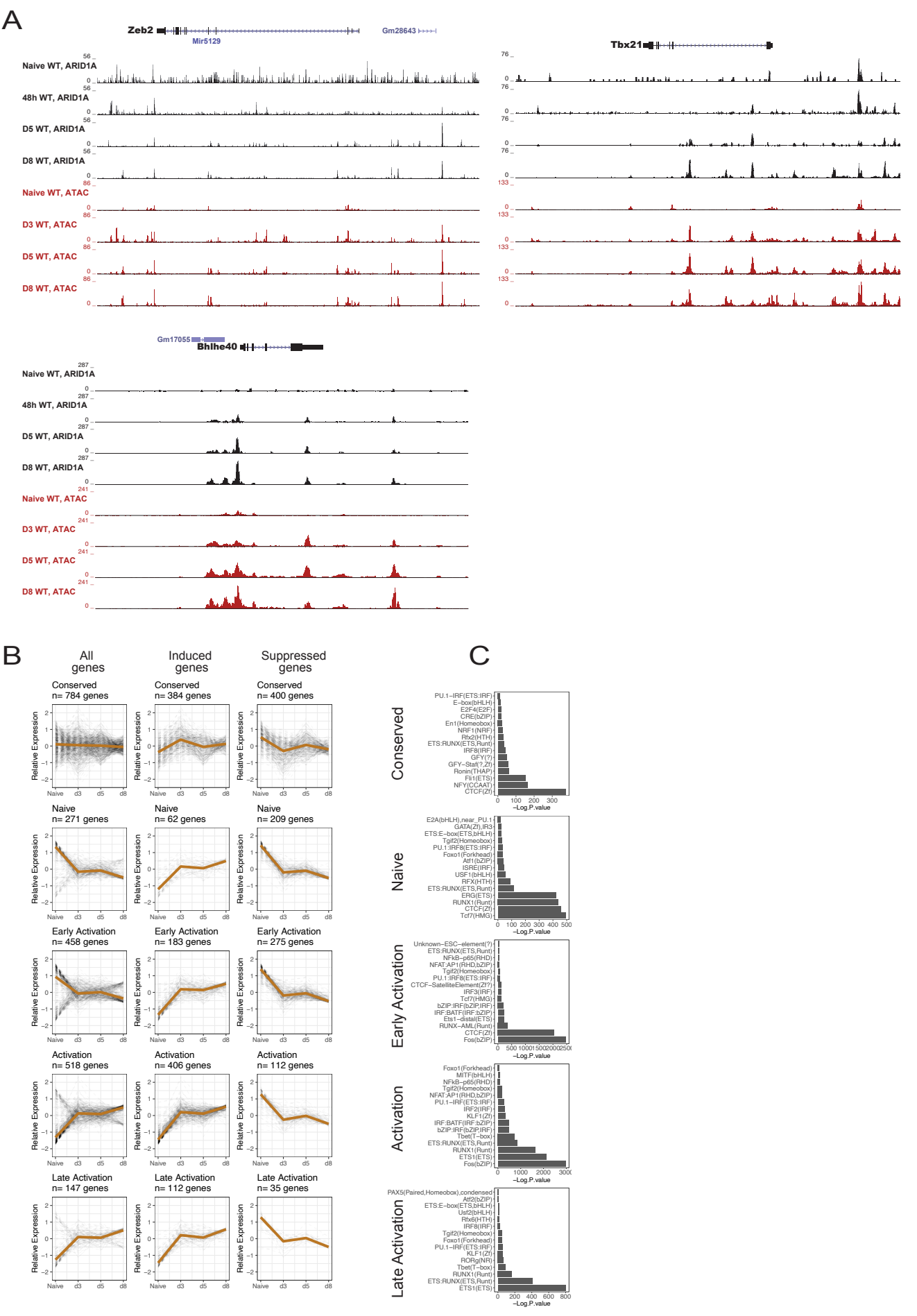
A
Zeb2
Mir5129
Gm28643
Naive WT, ARID1A
48h WT, ARID1A
D5 WT, ARID1A
D8 WT, ARID1A
Naive WT, ATAC
D3 WT, ATAC
D5 WT, ATAC
D8 WT, ATAC
Tbx21
Gm17055
Bhlhe40
B
All genes
Induced genes
Suppressed genes
Conserved
n= 784 genes
n= 384 genes
n= 400 genes
Naive
n= 271 genes
n= 62 genes
n= 209 genes
Early Activation
n= 458 genes
n= 183 genes
n= 275 genes
Activation
n= 518 genes
n= 406 genes
n= 112 genes
Late Activation
n= 147 genes
n= 112 genes
n= 35 genes
Relative Expression
Naive
d3
d5
d8
C
Conserved
PU.1−IRF(ETS:IRF)
E−box(bHLH)
E2F4(E2F)
CRE(bZIP)
En1(Homeobox)
NRF1(NRF)
Rfx2(HTH)
ETS:RUNX(ETS,Runt)
IRF8(IRF)
GFY(?)
GFY−Staf(?,Zf)
Ronin(THAP)
Fli1(ETS)
NFY(CCAAT)
CTCF(Zf)
−Log.P.value
Naive
E2A(bHLH),near_PU.1
GATA(Zf),IR3
ETS:E−box(ETS,bHLH)
Tgif2(Homeobox)
PU.1:IRF8(ETS:IRF)
Foxo1(Forkhead)
Atf1(bZIP)
ISRE(IRF)
USF1(bHLH)
RFX(HTH)
ETS:RUNX(ETS,Runt)
ERG(ETS)
RUNX1(Runt)
CTCF(Zf)
Tcf7(HMG)
Early Activation
Unknown−ESC−element(?)
ETS:RUNX(ETS,Runt)
NFkB−p65(RHD)
NFAT:AP1(RHD,bZIP)
Tgif2(Homeobox)
PU.1:IRF8(ETS:IRF)
CTCF−SatelliteElement(Zf?)
IRF3(IRF)
Tcf7(HMG)
bZIP:IRF(bZIP,IRF)
IRF:BATF(IRF:bZIP)
Ets1−distal(ETS)
RUNX−AML(Runt)
CTCF(Zf)
Fos(bZIP)
Activation
Foxo1(Forkhead)
MITF(bHLH)
NFkB−p65(RHD)
Tgif2(Homeobox)
NFAT:AP1(RHD,bZIP)
PU.1−IRF(ETS:IRF)
IRF2(IRF)
KLF1(Zf)
IRF:BATF(IRF:bZIP)
bZIP:IRF(bZIP,IRF)
Tbet(T−box)
ETS:RUNX(ETS,Runt)
RUNX1(Runt)
ETS1(ETS)
Fos(bZIP)
Late Activation
PAX5(Paired,Homeobox),condensed
Atf2(bZIP)
ETS:E−box(ETS,bHLH)
Usf2(bHLH)
Rfx6(HTH)
IRF8(IRF)
Tgif2(Homeobox)
Foxo1(Forkhead)
PU.1−IRF(ETS:IRF)
KLF1(Zf)
RORg(NR)
Tbet(T−box)
RUNX1(Runt)
ETS:RUNX(ETS,Runt)
ETS1(ETS)

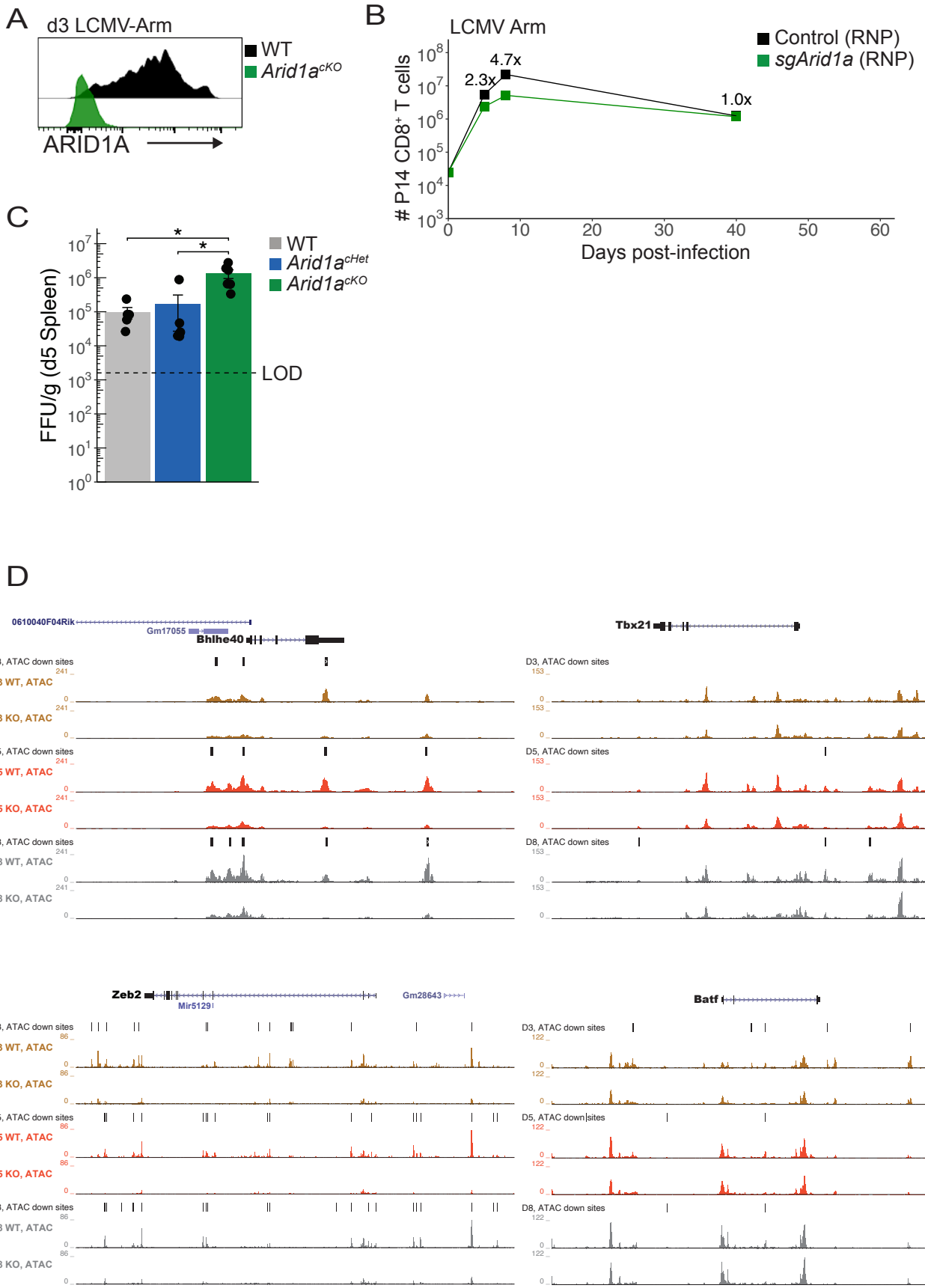
A
d3 LCMV-Arm
WT
Arid1a^cKO
ARID1A
B
LCMV Arm
Control (RNP)
sgArid1a (RNP)
P14 CD8+ T cells
4.7x
2.3x
1.0x
Days post-infection
C
WT
Arid1a^cHet
Arid1a^cKO
FFU/g (d5 Spleen)
LOD
D
0610040F04Rik
Gm17055
Bhlhe40
Tbx21
Tbkbp1
Zeb2
Mir5129
Gm28643
Batf
D3, ATAC down sites
D3 WT, ATAC
D3 KO, ATAC
D5, ATAC down sites
D5 WT, ATAC
D5 KO, ATAC
D8, ATAC down sites
D8 WT, ATAC
D8 KO, ATAC

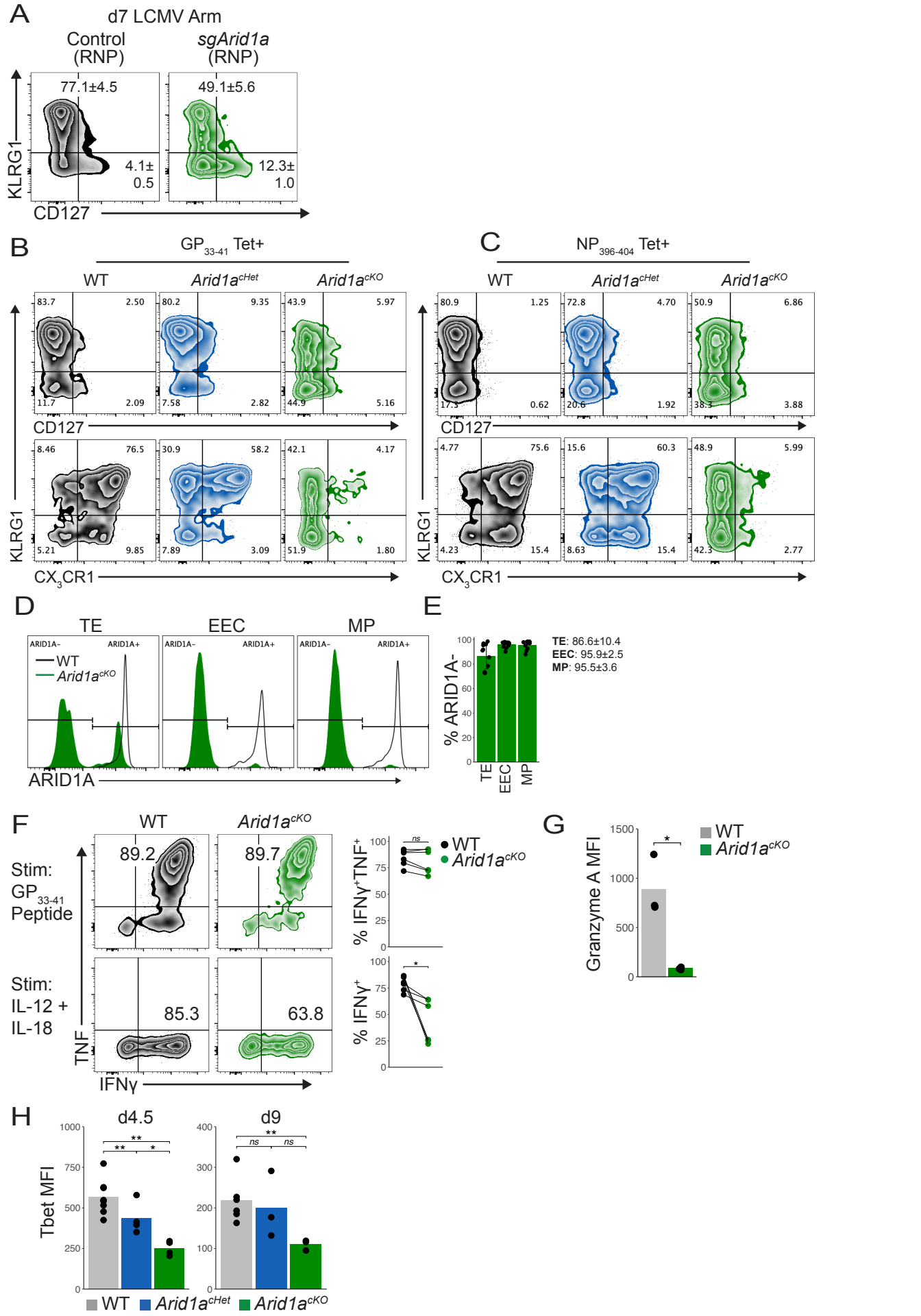
A
d7 LCMV Arm
Control (RNP)
sgArid1a (RNP)
77.1±4.5
4.1± 0.5
49.1±5.6
12.3± 1.0
KLRG1
CD127
B
GP33-41 Tet+
WT
Arid1acHet
Arid1acKO
83.7
2.50
11.7
2.09
80.2
9.35
7.58
2.82
43.9
5.97
44.9
5.16
8.46
76.5
5.21
9.85
30.9
58.2
7.89
3.09
42.1
4.17
51.9
1.80
CD127
KLRG1
CX3CR1
C
NP396-404 Tet+
WT
Arid1acHet
Arid1acKO
80.9
1.25
17.3
0.62
72.8
4.70
20.6
1.92
50.9
6.86
38.3
3.88
4.77
75.6
4.23
15.4
15.6
60.3
8.63
15.4
48.9
5.99
42.3
2.77
CD127
KLRG1
CX3CR1
D
TE
EEC
MP
ARID1A-
ARID1A+
WT
Arid1acKO
ARID1A
E
% ARID1A-
TE
EEC
MP
TE: 86.6±10.4
EEC: 95.9±2.5
MP: 95.5±3.6
F
WT
Arid1acKO
Stim: GP33-41 Peptide
Stim: IL-12 + IL-18
89.2
89.7
85.3
63.8
TNF
IFNγ
% IFNγ+TNF+
% IFNγ+
ns
*
WT
Arid1acKO
G
Granzyme A MFI
*
WT
Arid1acKO
H
d4.5
d9
Tbet MFI
**
*
ns
WT
Arid1acHet
Arid1acKO

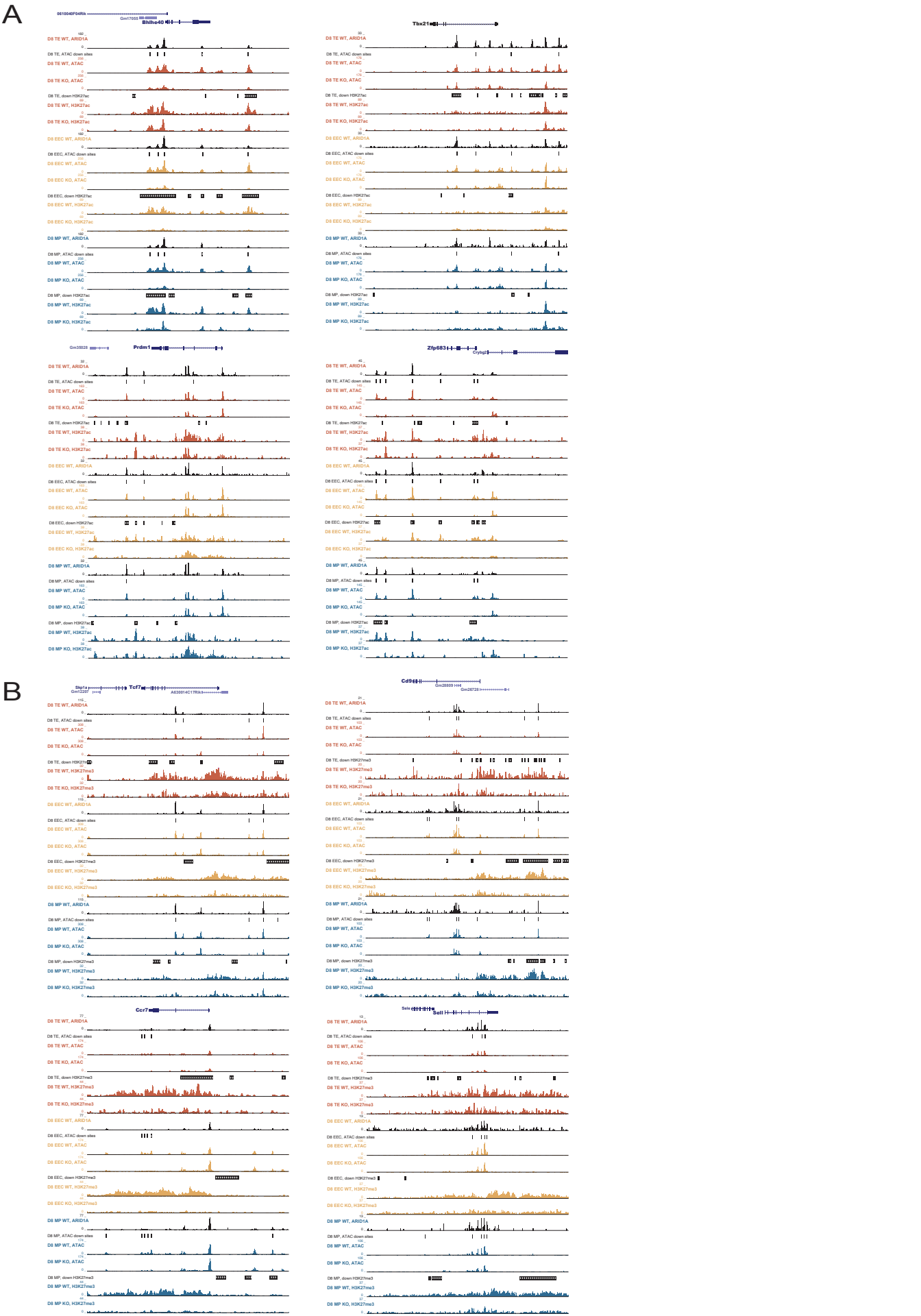
A
Bhlhe40
Tbx21
Prdm1
Zfp683
B
Tcf7
Cd9
Ccr7
Sell

A

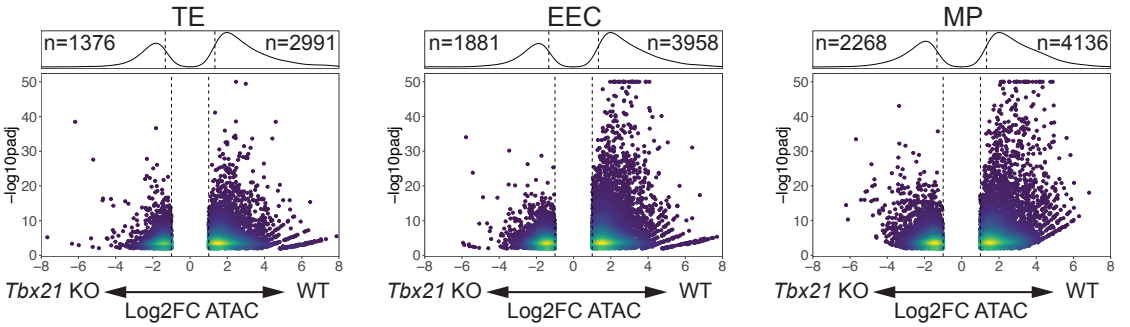

B

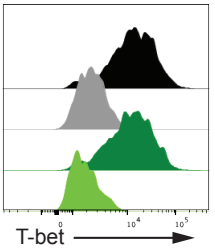

Genotype	Tbet-OE	Tbet MFI
WT	+	11885
WT	-	2424
Arid1a^{cKO}	+	10570
Arid1a^{cKO}	-	1828

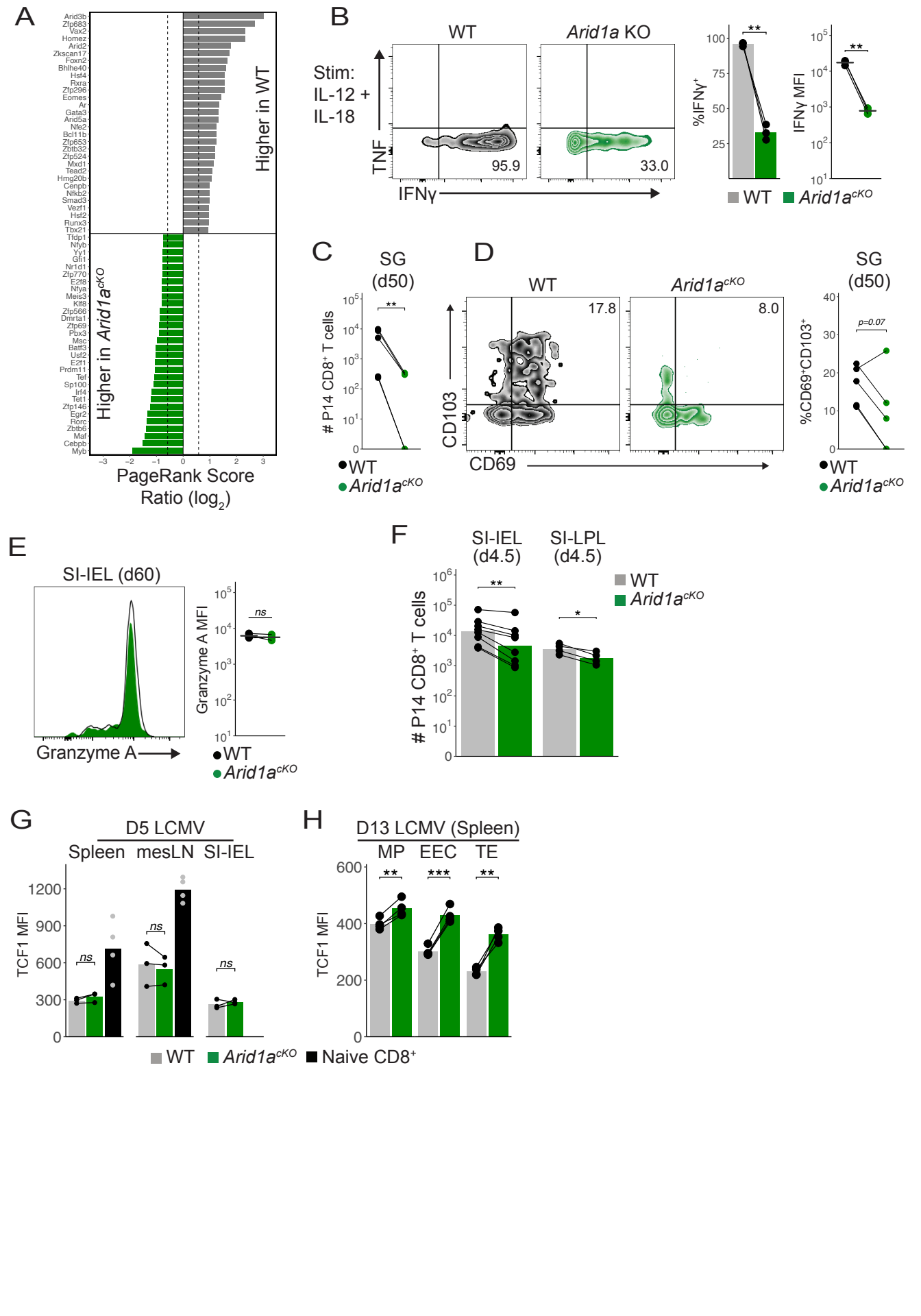
A
Higher in WT
Higher in Arid1a cKO
PageRank Score Ratio (log2)
B
WT
Arid1a KO
Stim: IL-12 + IL-18
TNF
IFNγ
95.9
33.0
%IFNγ+
IFNγ MFI
WT
Arid1acKO
C
SG (d50)
P14 CD8+ T cells
WT
Arid1acKO
D
WT
Arid1acKO
17.8
8.0
CD103
CD69
SG (d50)
%CD69+CD103+
p=0.07
E
SI-IEL (d60)
Granzyme A
Granzyme A MFI
ns
F
SI-IEL (d4.5)
SI-LPL (d4.5)
P14 CD8+ T cells
G
D5 LCMV
Spleen
mesLN
SI-IEL
TCF1 MFI
Naive CD8+
H
D13 LCMV (Spleen)
MP
EEC
TE
TCF1 MFI

Figure S1. Chromatin accessibility and ARID1A binding in antiviral CD8$^+$ T cells, related to Figure 1

(A) ARID1A CUT&RUN and ATAC-seq signal tracks at *Zeb2*, *Tbx21*, and *Bhlhe40*. (B) Relative gene expression of genes annotated to OCR clusters in Fig 1A. Naïve samples are from GSE152841. (C) Top 15 motifs enriched in OCR clusters.

Figure S2. ARID1A regulates accessibility of effector-associated TFs, related to Figure 2

(A) Confirmation of efficient ARID1A deletion at 72h post-infection in *Arid1a*^{cKO} P14 spleen cells. (B) Numbers of control RNP or sg*Arid1a* RNP P14 cells following LCMV-Armstrong infection. (C) LCMV titers in the spleen of WT (n=5), *Arid1a*^{cHet} (n=6), and *Arid1a*^{cKO} (n=6) mice d5 p.i. (D) ATAC-seq signal tracks at *Bhlhe40*, *Tbx21*, *Zeb2*, and *Batf.*. LOD; limit of detection. *p<0.05.

Figure S3. *Arid1a* KO antiviral CD8$^+$ T cells are developmentally and functionally impaired, related to Figure 3

(A) TE and MP cells in control or sg*Arid1a* RNP (*Arid1a* KO) P14 cells at 7d post-infection. Mean ± SEM of TE (KLRG1$^+$CD127$^-$) and MP (KLRG1$^-$CD127$^+$) cells are shown. (B) GP_{33}- and (C) NP_{396}-tetramer$^+$ endogenous CD8$^+$ T cells at d8 post-infection. (D,E) ARID1A deletion efficiency in d8-d10 *Arid1a*^{cKO} effector subsets (n=11). Mean ± SEM of ARID1A-deleted cells are shown for each subset. (F) Cytokine production from WT or *Arid1a*^{cKO} P14 cells 7-8 days post-infection stimulated with either GP33 peptide or IL-12 and IL-18. Representative flow plots show the frequency of IFNg$^+$TNF$^+$ (top) cells after peptide stimulation and frequency of IFNg$^+$ (bottom) cells after IL-12 and IL-18 stimulation. Paired t-test. (G) Granzyme A staining in WT and *Arid1a* P14 cells at d8 p.i. (H) T-bet staining in WT, *Arid1a*^{cHet}, and *Arid1a*^{cKO} effector cells at d4.5 or d9 post-infection. *ns*, not significant; *p<0.05, **p<0.005

Figure S4. ARID1A regulates accessibility and deposition of histone modifications, related to Figure 4

(A) ATAC-seq and H3K27ac CUT&RUN signal tracks at (A) *Bhlhe40*, *Tbx21*, *Prdm1,* and *Zfp683*. (B) ATAC-seq and H3K27me3 CUT&RUN signal tracks at *Tcf7*, *Cd9*, *Ccr7*, and *Sell*.

Figure S5. T-bet regulates chromatin accessibility profiles in effector CD8$^+$ T cells, related to Figure 5

(A) Differential accessibility analysis of WT and *Tbx21* KO TE, EEC, and MP P14 cells at d8 p.i. Numbers of differentially accessible peaks are shown (Fold change ≥ 2, adjusted p value < 0.01, Benjamini-Hochberg). (B) T-bet expression in WT and *Arid1a*^{cKO} cells transduced with control or T-bet overexpression retrovirus and cultured *in vitro* for 72h.

Figure S6. ARID1A promotes Trm formation, related to Figure 6

(A) Taiji PageRank TF score ratios in WT versus *Arid1a*^{cKO} MP cells. The top 30 TFs with a threshold ratio of fold change > 1.5 in each direction are shown. (B) IFNγ production by WT and *Arid1a*^{cKO} memory P14 cells stimulated with IL-12 and IL-18 *in vitro* at d60 post-infection. (C) Absolute numbers and (D) CD69/CD103 expression profiles of IV- WT and *Arid1a* KO salivary gland Trm cells at d50 post-infection. (E) Granzyme A staining in WT and *Arid1a*^{cKO} SI-IEL Trm. (F) Absolute numbers of WT and *Arid1a*^{cKO} SI-IEL and SI-LPL cells at d4.5 p.i. (G) TCF1 expression in naïve WT CD8$^+$ T cells and WT or *Arid1a*^{cKO} effector cells 5d p.i in spleen, mesenteric lymph node (mesLN), and SI-IEL. (H) TCF1 expression in WT and

Arid1a^{cKO} MP, EEC, and TE cells 13d p.i. Paired t-test was used in cases where line connects observations. *ns*, not significant; *p<0.05, **p<0.005, ***p<0.0005.